American Mineralogist, Volume 74, pages 750–758, 1989

Composition of volcanic allanite from the Toba Tuffs, Sumatra, Indonesia

Craig A. Chesner
Department of Geological Engineering, Geology, and Geophysics, Michigan Technological University, Houghton, Michigan 49931, U.S.A.
Art D. Ettlinger
Department of Geology, Washington State University, Pullman, Washington 99164, U.S.A.

Abstract

The crystal-rich, chemically zoned Toba Tuffs commonly contain accessory allanite. Electron-microprobe analyses of this LREE-rich phase exhibit significant variations that correlate generally with magmatic evolution and temperature. Allanite compositions from the different Toba Tuffs mostly overlap, although selected elements allow distinction among the units. Fractionation of allanite from the Toba magmas can be demonstrated from bulk-rock and glass INAA. Crystal/liquid distribution coefficients permit calculation of fractionated proportions and modal abundances. Toba Tuffs that erupted below 800 °C contain allanite regardless of bulk-rock composition, whereas samples that erupted above 800 °C contain none. Bishop Tuff allanites generally have higher concentrations of LREEs than Toba's, even though their bulk rocks have lower LREE abundances. Apparently temperature is a critical factor that influences allanite crystallization, and magmatic LREE concentrations are of little importance.

Introduction

The largest Quaternary volcanic eruption on Earth occurred in northern Sumatra 75000 years ago from the Toba caldera complex (Fig. 1). This eruption was the fourth ignimbrite-forming eruption from Toba in the past 1.2 m.y. These eruptions have left a 100 × 30 km caldera complex that parallels the active volcanic front of Sumatra. From oldest to youngest, the four tuffs erupted from Toba include the 1.2 Ma Haranggoal Dacite Tuff (HDT), followed by the 0.84 Ma Oldest Toba Tuff (OTT), the 0.50 Ma Middle Toba Tuff (MTT), and finally the 75 ka Youngest Toba Tuff (YTT) (Knight et al., 1986; Chesner, unpublished data). Of these, the three youngest tuffs are compositionally zoned from calc-alkalic rhyolite (76% SiO_2) to quartz latite (68% SiO_2) (Chesner, 1985). The compositional zonation of these rocks can be shown to originate mostly from crystal fractionation of the wide variety of mineral phases in Toba rocks. Crystal contents as high as 40 wt% consist of quartz, sanidine, plagioclase, biotite, and amphibole, with minor orthopyroxene, magnetite, ilmenite, fayalite, zircon, and allanite. Inclusions of apatite occur in most phases, and pyrrhotite was noted in Fe-Ti oxides and zircon. Of particular interest is the occurrence of allanite, which is rare or absent in most volcanic rocks, but abundant at Toba. Marel (1948) noted that allanite can be used as a characteristic guide mineral of the Toba Tuffs on eastern Sumatra.

Although accessory allanite has been noted in various igneous and metamorphic rocks, chemical descriptions are scarce. Exley (1980), Gromet and Silver (1983), and Michael (1984) reported electron-microprobe analyses of allanites from Skye granites, a granodiorite from the Peninsular batholith of California, and the Cordilleran Paine granite of southern Chile, respectively. A metamorphic occurrence in British Columbia has been described by Campbell and Ethier (1984). Volcanic allanite has been described from the Bishop Tuff in California by Hildreth (1977, 1979) and from the Sandy Braes welded tuff of Northern Ireland by Brooks et al. (1981). This paper describes the character and composition of allanites from the Toba Tuffs, discusses crystallization and fractionation effects, evaluates crystal/liquid distribution coefficients, and compares the allanite of the Toba Tuffs with other volcanic occurrences described in the literature.

Analytical techniques

Allanite was separated by heavy liquids and concentrated magnetically. Polished mineral mounts were prepared, and wavelength-dispersive analyses were performed with a Cameca electron microprobe at Washington State University. Operating conditions and standards used appear in Table 1. Precision and accuracy are considered to be better than 1%, and detection limits are generally between 0.05 and 0.10 wt%. Selected allanite concentrates and associated glasses were also analyzed by INAA at Washington State University. Samples were analyzed for La, Ce, Sm, Eu, Tb, Yb, and Lu. Gamma-ray energies were counted on a GE (Li) high-resolution spectrometer. Analyzed concentrations for these elements are well above detection limits and generally precise and accurate within 5%.

0003–004X/89/0708–0750$02.00

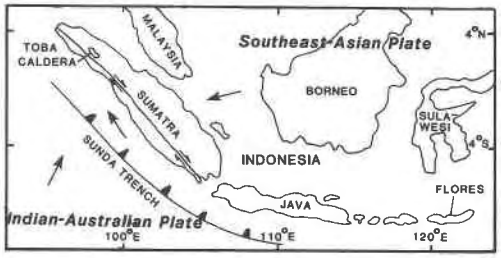

Fig. 1. Tectonic and location map of the Toba caldera.

Petrography

Allanite is present in thin sections from the three youngest tuffs erupted at Toba regardless of their bulk-rock composition (Fig. 2). It also occurs in a few post-YTT lava domes but is absent from the HDT. Phenocrysts are commonly euhedral, twinned, up to 0.5 mm in length, and pleochroic from deep red-brown to light green. Refractive indices determined by Marel (1948) are $\alpha = 1.73$, $\beta = 1.74$, and $\gamma = 1.75$. Abundant apatite rods and needles and less commonly magnetite and zircon are included in the phenocrysts. Negative crystal-melt inclusions up to 0.05 mm occur in most phenocrysts. Multiple inclusion sets occur where an allanite has apatite or zircon inclusions that contain an inclusion with a vapor bubble. Whether these smallest inclusions are also apatites or zircons or are negative-crystal melt inclusions has not been established, but the presence of the vapor bubble suggests that most are melt inclusions.

Table 1. Standards used for WDS electron-microprobe analyses of Toba allanite

Element	Standard
Si	Quartz
Ti	Sphene
Al	REE-3*
Fe	Hematite
Mn	Spessartine
Mg	Olivine
Ca	Diopside
Y	REE-3*
La	REE-3*
Ce	CeO_2*
Pr	REE-3*
Nd	REE-2*
Sm	REE-2*
Th	ThO_2*

Note: 25-kV accelerating voltage; 8-μm beam diameter; standard ZAF data reduction.
* Synthetic standards: REE-2, REE-3 from Drake and Weill (1972).

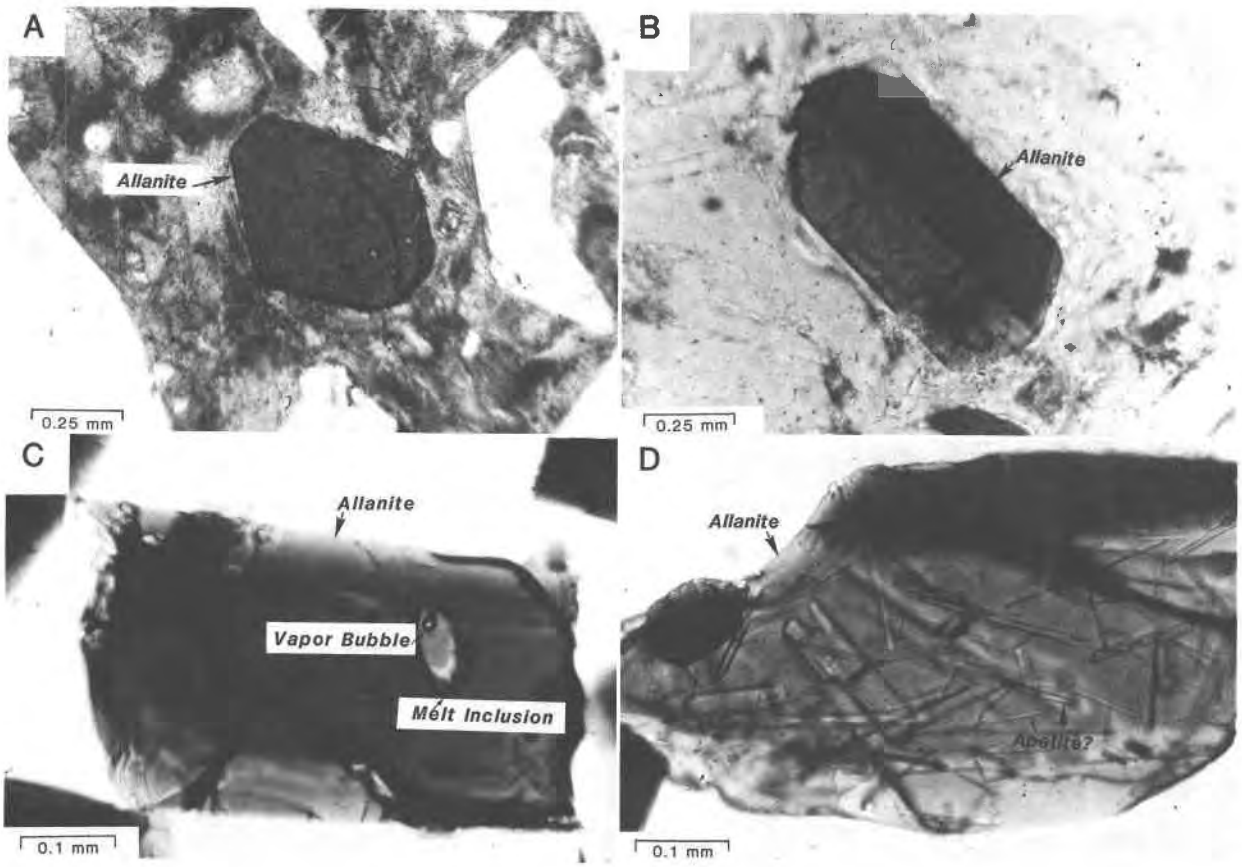

Fig. 2. Photomicrographs of Toba allanite. (**A**) Euhedral phenocryst in welded tuff. (**B**) Twinned phenocryst in incipiently welded tuff. (**C**) Melt inclusion with vapor bubble. (**D**) Apatite? and/or zircon inclusions in allanite.

Table 2. Representative allanite electron-microprobe analyses and structural formulas from the Toba Tuffs

	OTT			MTT			YTT			Domes	
	16-1	74-1	32B-1	8-1	7-2	99-2	51A5-2	84A4-2	89A2-2	67-1	3-1
SiO_2	32.61	32.24	32.96	31.40	31.67	32.36	31.21	32.55	31.74	30.92	32.00
TiO_2	0.89	0.98	0.89	0.78	1.49	1.24	0.90	0.96	1.08	1.01	0.96
Al_2O_3	13.99	14.12	14.88	13.70	13.75	14.11	13.15	13.87	14.05	12.99	14.21
Fe_2O_3	3.04	3.57	2.77	2.81	3.48	2.11	4.36	3.18	3.42	5.12	3.42
FeO	12.83	11.78	11.87	13.57	11.58	12.48	11.56	11.96	11.01	10.66	11.02
MnO	0.66	0.42	0.36	0.67	0.24	0.30	0.99	0.62	0.37	0.72	0.42
MgO	0.84	0.94	1.15	0.41	1.00	1.15	0.90	1.12	1.33	1.01	1.20
CaO	9.95	10.44	10.52	9.13	10.40	9.93	9.54	10.17	10.17	10.12	10.42
Y_2O_3	0.29	0.13	0.10	0.48	0.16	0.14	0.43	0.20	0.07	0.27	0.05
La_2O_3	5.77	6.93	7.38	4.80	7.13	7.43	5.95	6.82	7.61	6.41	7.11
Ce_2O_3	11.25	11.73	11.69	10.81	12.09	12.16	11.76	11.76	11.98	11.51	11.71
Pr_2O_3	1.09	1.11	0.90	1.21	1.15	1.00	1.17	0.97	1.01	1.08	0.98
Nd_2O_3	3.61	3.00	2.64	4.51	3.36	2.93	3.83	3.09	2.85	3.41	2.67
Sm_2O_3	0.47	0.25	0.24	0.80	0.25	0.18	0.46	0.37	0.13	0.35	0.19
ThO_2	1.75	1.37	1.03	2.17	0.56	0.89	1.83	1.35	0.93	1.73	0.87
Total	99.04	99.01	99.38	97.25	98.31	98.41	98.04	98.99	97.75	97.31	97.23
Si	3.109	3.074	3.098	3.087	3.048	3.100	3.051	3.103	3.061	3.032	3.081
Ti	0.064	0.070	0.063	0.058	0.108	0.089	0.066	0.069	0.078	0.074	0.070
Al	1.573	1.587	1.649	1.588	1.560	1.594	1.516	1.559	1.597	1.502	1.613
Fe^{3+}	0.218	0.256	0.196	0.208	0.252	0.152	0.320	0.228	0.248	0.378	0.248
Fe^{2+}	1.023	0.939	0.933	1.116	0.932	1.000	0.945	0.953	0.888	0.874	0.887
Mn	0.053	0.034	0.029	0.056	0.020	0.024	0.082	0.050	0.030	0.060	0.034
Mg	0.119	0.134	0.161	0.060	0.143	0.164	0.131	0.159	0.191	0.148	0.172
Total	3.050	3.020	3.031	3.086	3.015	3.023	3.060	3.018	3.032	3.036	3.024
Ca	1.017	1.067	1.059	0.962	1.073	1.019	0.999	1.039	1.051	1.063	1.075
Y	0.015	0.007	0.005	0.025	0.008	0.007	0.022	0.010	0.004	0.014	0.003
La	0.203	0.244	0.256	0.174	0.253	0.263	0.215	0.240	0.271	0.232	0.252
Ce	0.393	0.410	0.402	0.389	0.426	0.427	0.421	0.410	0.423	0.413	0.413
Pr	0.038	0.039	0.031	0.043	0.040	0.035	0.042	0.034	0.035	0.039	0.034
Nd	0.123	0.102	0.089	0.158	0.116	0.100	0.134	0.105	0.098	0.119	0.092
Sm	0.015	0.008	0.008	0.027	0.008	0.006	0.015	0.012	0.004	0.012	0.006
Th	0.038	0.030	0.022	0.049	0.012	0.019	0.041	0.029	0.020	0.039	0.019
Total	1.842	1.907	1.872	1.827	1.936	1.876	1.889	1.879	1.942	1.931	1.894

Composition

Allanite is a monoclinic member of the epidote group and has a general formula of $(Ca,REE,Th)_2(Fe^{2+}Fe^{3+}Al)_3Si_3O_{12}OH$. Dollase (1971) gave the site-specific general formula as $A_2M_3Si_3O_{12}OH$. In both epidote ($Ca_2Fe^{3+}Al_2Si_3O_{12}OH$) and allanite, the A(1) site is always filled by Ca^{2+}. However in allanite, Ca^{2+} in the larger A(2) site is substituted for by considerable amounts of REE^{3+}, Th^{4+}, Sr^{2+}, and possibly Mn^{2+}. Charge balance is maintained by the coupled substitution $Ca^{2+}_{A(2)}Fe^{3+}_{M(3)} = REE^{3+}_{A(2)}Fe^{2+}_{M(3)}$. Peacor and Dunn (1988) have shown that complete octahedral-site assignments and Fe^{2+}/Fe^{3+} estimates in allanite require F and H analyses. In the absence of these data, the octahedral sites in order of size are M(3) > M(1) > M(2). The M(3) and M(1) sites are occupied by Al^{3+}, Fe^{3+}, Fe^{2+}, Mn^{3+}, Ti^{4+}, and Mg^{2+}, and M(2) is filled by Al^{3+} (Dollase, 1971; Exley, 1980).

Electron-microprobe analyses

Approximately 70 allanite phenocrysts were analyzed by electron microprobe. Two or three phenocrysts were analyzed from each sample; these were chosen to represent the compositional variation of the allanite-bearing tuffs. In order to assess compositional zonation of individual phenocrysts, rims and cores of some crystals were analyzed. Structural formulas were calculated on the basis of 8 cations, and the total negative charge was then adjusted to 25, enabling estimation of the Fe^{2+}/Fe^{3+} ratio (Table 2). The average structural formula for the entire suite is given below.

$$(Ca_{1.045}Y_{0.010}La_{0.239}Ce_{0.409}Pr_{0.037}Nd_{0.109}Sm_{0.011}Th_{0.030})_{1.890}(Fe^{2+}_{0.935}Fe^{3+}_{0.259}Al_{1.572}Mn_{0.045}Mg_{0.151}Ti_{0.073})_{3.035}Si_{3.075}O_{12}OH$$

The average total of all analyses is 98.64%, which implies a water content of about 1.36%. Water content calculated for the above formula is 1.55%, and both estimates fall within the range for allanite reported by Deer et al. (1962) of 1.08–3.33%. Total rare-earth oxide contents exceed 23 wt%, and La and Ce are $>10^5$ times chondritic abundances.

INAA

Neutron-activation analyses were performed on three bulk samples and seven mineral separates of allanite and corresponding glasses that represent the three allanite-bearing Toba Tuffs (Tables 3a, and 3b). The INAA allanite data represent minimum concentrations because of the

TABLE 3A. INAA of allanite separates (given in ppm, unless designated otherwise)

	YTT		MTT		OTT		
	21A5A	94A5A	8A	7A	15AA	27A	74A
La	12690	48000	38820	46280	110 300	38190	43360
Ce	21110	77060	76850	85590	82 630	76000	86870
Sm	466	2061	1836	3109	6 055	1993	1999
Eu	18.9	45.3	68.9	68.9	41.9	41.2	46.8
Tb	14	63	56	86	83	77	75
Yb	21	103	97	136	143	146	149
Lu	2.80	11.91	9.11	13.3	12.59	16.20	16.62
La_2O_3 (%)	1.49	5.63	4.55	5.43	12.94	4.48	5.09
Ce_2O_3 (%)	2.47	9.03	9.00	10.03	9.68	8.90	10.18
Sm_2O_3 (%)	0.05	0.24	0.21	0.36	0.70	0.23	0.23

Note: Because of significant deviation from other samples, 21A5A and 15AA are not considered representative of Toba allanite.

TABLE 3B. INAA of glasses associated with allanite separates listed in Table 3a as well as several bulk-rock analyses

	Glasses							Bulk-rock		
	YTT		MTT		OTT			YTT		
	21A5G	94A5G	8G	7G	15AG	27G	74G	21A5	63A1	20A2
La	51.66	21.10	35.14	22.69	nd	23.18	28.90	52.1	63.8	32.2
Ce	90.68	56.42	82.21	64.44	61.10	62.62	67.56	129.8	111.7	61.9
Sm	4.54	3.89	4.15	3.85	nd	4.08	4.11	5.76	6.15	3.97
Eu	0.75	0.28	0.75	0.60	0.48	0.48	0.90	1.65	1.31	0.49
Tb	0.49	0.59	0.52	0.62	0.72	0.61	0.58	0.36	0.99	0.78
Yb	3.49	5.55	3.17	3.73	5.42	5.02	3.96	3.43	3.10	4.49
Lu	0.63	0.96	0.51	0.57	0.98	0.86	0.66	0.68	0.51	0.66

Note: Analyses arranged in order of increasing bulk-rock silica content from left to right for each unit.

presence of abundant inclusions and impure mineral separations. The INAA concentrations are systematically about 20% lower than the electron-microprobe data. This shows that the separates are only about 80% allanite. Accordingly, the allanite electron-microprobe analyses are assumed to be more reliable. Using all data, the Ce/Yb ratio of Toba allanites may be as high as 1000, demonstrating their extreme LREE enrichment.

DISCUSSION

Chemical variation of Toba allanites

Individual allanite phenocrysts in all units are compositionally zoned but not systematically. Allanite composition varies within each unit and between different units (Fig. 3). Chemical variation is greatest within the MTT, while the OTT varies the least. Interunit variations are clearest in the MnO vs. MgO plot, which separates the units into distinct fields. Commonly, for each unit, allanites plotting at one end are from the most silicic rocks, erupted at temperatures between 710 and 730 °C (Fe-Ti oxide temperature from Chesner and Rose, 1987). Allanites separated from less-evolved rocks, erupted at 730–770 °C, plot at the opposite end of each field. Compositionally, the portion of each field associated with the most silicic rocks contains allanites with the highest FeO and MnO contents and the lowest MgO and TiO_2. Also, these allanites often have higher Y_2O_3, Pr_2O_3, Nd_2O_3, Sm_2O_3, and ThO_2 at the expense of La_2O_3 and Ce_2O_3 than allanites from the less-evolved rocks. Such correlations suggest that allanite composition depends upon either the temperature or composition of the zoned Toba magmas, or both. In addition, since all allanite-bearing Toba tuffs have similar temperature and chemical ranges, slight differences in P_{total} and P_{H_2O} between units may contribute to the distinct compositions of their allanites. Coupled substiutution of $CaO + ThO_2$ in the A structural site decreases as REE abundances increase (Fig. 4). The OTT has the lowest REE abundances and the MTT the highest.

Allanite fractionation

Petrographic evidence suggests that allanite is a liquidus phase in the three youngest Toba tuffs. Since it is present within the compositional range from 68% to 76% SiO_2, we can assume that it was a fractionating phase during most of the magmatic evolution at Toba. The effect of fractionating allanite from the Toba magmas before eruption can be evaluated by comparing the REE abundances of allanite samples and their associated glass separates. In Figure 5, the glasses separated from the least-evolved rocks have the highest LREE and lowest HREE abundances. This results in a "cross-over" in the REE patterns between Eu and Tb, illustrating that allanite fractionation causes the LREEs to behave compatibly in the magma. Although the HREEs have crystal/liquid distribution coefficients greater than one in allanite (Table 4), they are incompatible in the Toba magmas because of their low concentrations (compared to LREEs) in allanite and their exclusion from other dominant fractionating

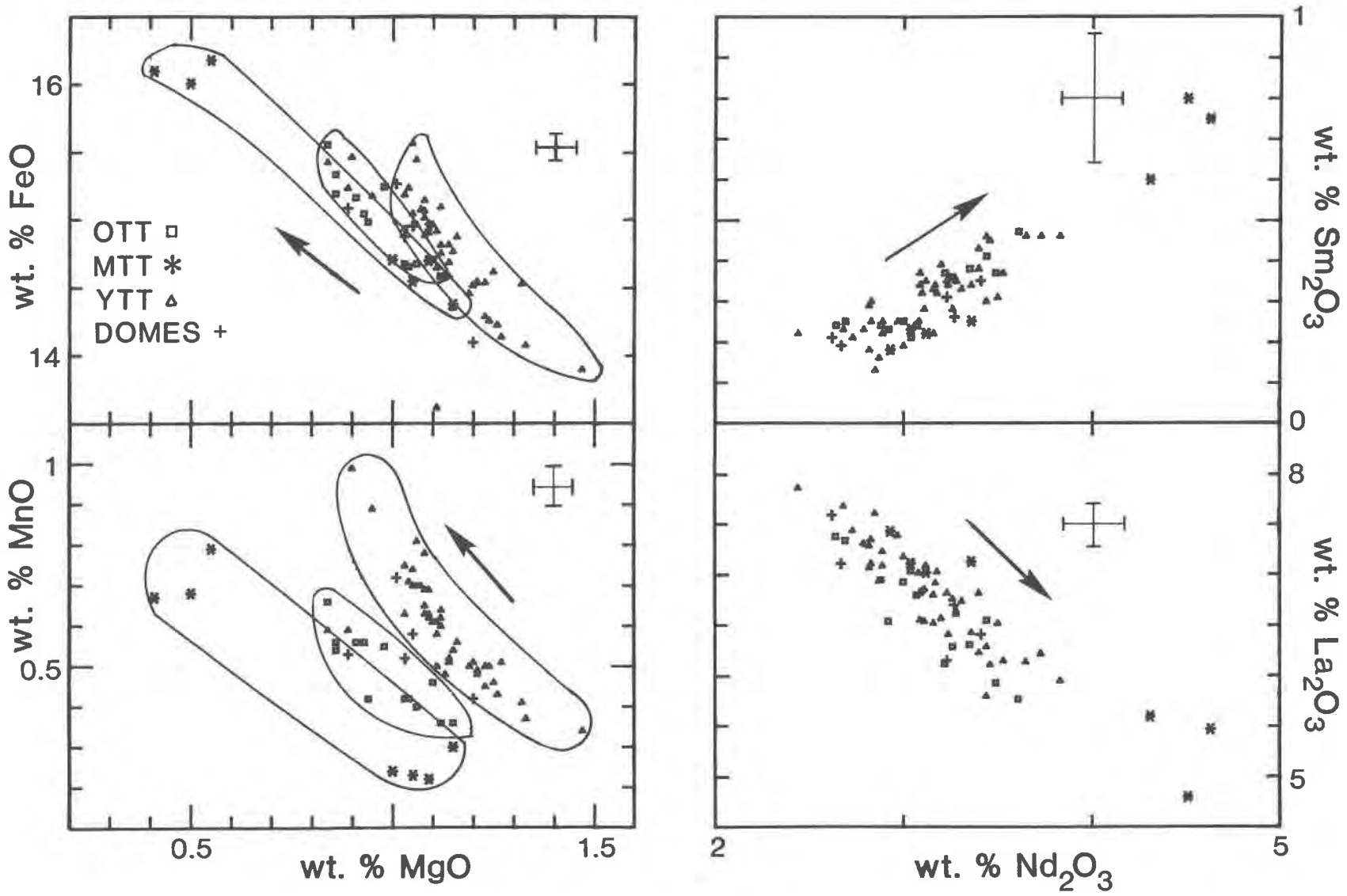

Fig. 3. Selected variation diagrams for individual allanite analyses. Symbols denote allanite from different eruptive units. All Fe as FeO. Arrows indicate the general trend toward lower temperatures and greater magmatic evolution within each unit as indicated by Fe-Ti oxides and bulk-rock chemistry.

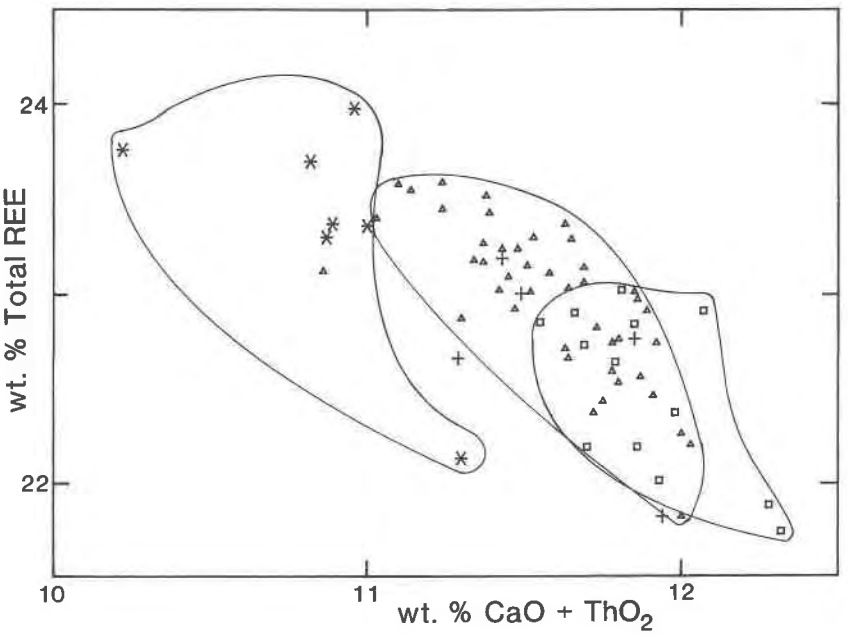

Fig. 4. Plot of total REEs vs. CaO + ThO_2 suggesting coupled substitution in the A structural site. Symbols are same as in Fig. 3.

phases. Michael (1983) and Cameron (1984) have shown that allanite fractionation was responsible for similar behavior of REEs in the Bishop Tuff. Thus, the compatible behavior of the LREEs in the Toba glass and bulk-rock data are strong evidence for allanite fractionation.

Assuming that the majority of the LREEs of the Toba magmas resided in either the liquid or allanite, it is possible to use Rayleigh calculations to determine the amount of allanite fractionation necessary to produce the observed LREE concentrations in the bulk rock. Crystal/liquid distribution coefficients from Table 4 are used to calculate allanite fractionation. About 0.052% modal fractionation can account for the observed decreases in La, Ce, and Sm from low-SiO_2 to the high-SiO_2 magmas of the YTT. This technique also allows calculation of the allanite modes. A low-SiO_2 YTT pumice (T-21A5) contains about 0.035% modal allanite whereas a high-SiO_2 pumice (T-94A5) has only about 0.016%. This illustrates that fractionation of small amounts of accessory phases rich in REEs can control REE patterns. With such minor modal abundances, presence of accessory phases could easily be missed petrographically. Such oversights could have major effects on petrologic models of tuffs other than Toba.

Temperature

Hildreth (1979) demonstrated that allanite did not begin to crystallize in the Bishop Tuff until the magma reached a critical temperature of 800 °C [Fe-Ti oxide temperature corrected from 763 °C with Andersen and Lindsley's (1985) revised data]. Allanite-bearing Toba tuffs were all erupted at temperatures of 710–770 °C, which are below the critical allanite temperature established by Hildreth. The HDT and some post-YTT domes lack allanite. These are the least-silicic Toba rocks (65–67% SiO_2) and also the hottest (810–870 °C). Therefore, the Toba data are consistent with the concept of a critical saturation temperature of about 800 °C for allanite crystallization in silicic magmas.

The REE abundances in the Toba Tuffs and the Bishop Tuff are not anomalous for calc-alkalic magmas. We propose that allanite in igneous rocks does not crystallize as a result of abnormal or elevated REE abundances, but

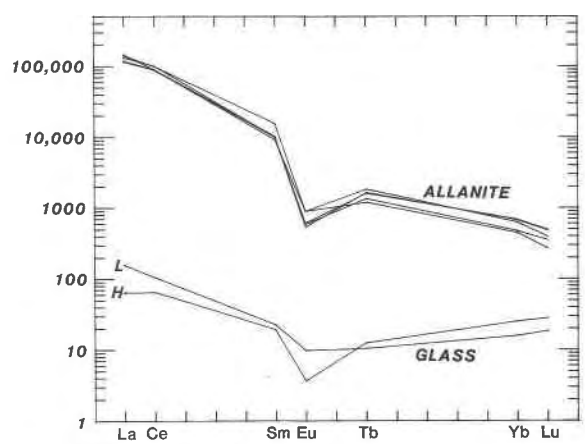

Fig. 5. REE plot of Toba allanite separates and two associated glasses, normalized to chondrite. L and H represent glasses separated from low- and high-SiO_2 bulk-rock samples, respectively. Other associated glasses not plotted fall within this range.

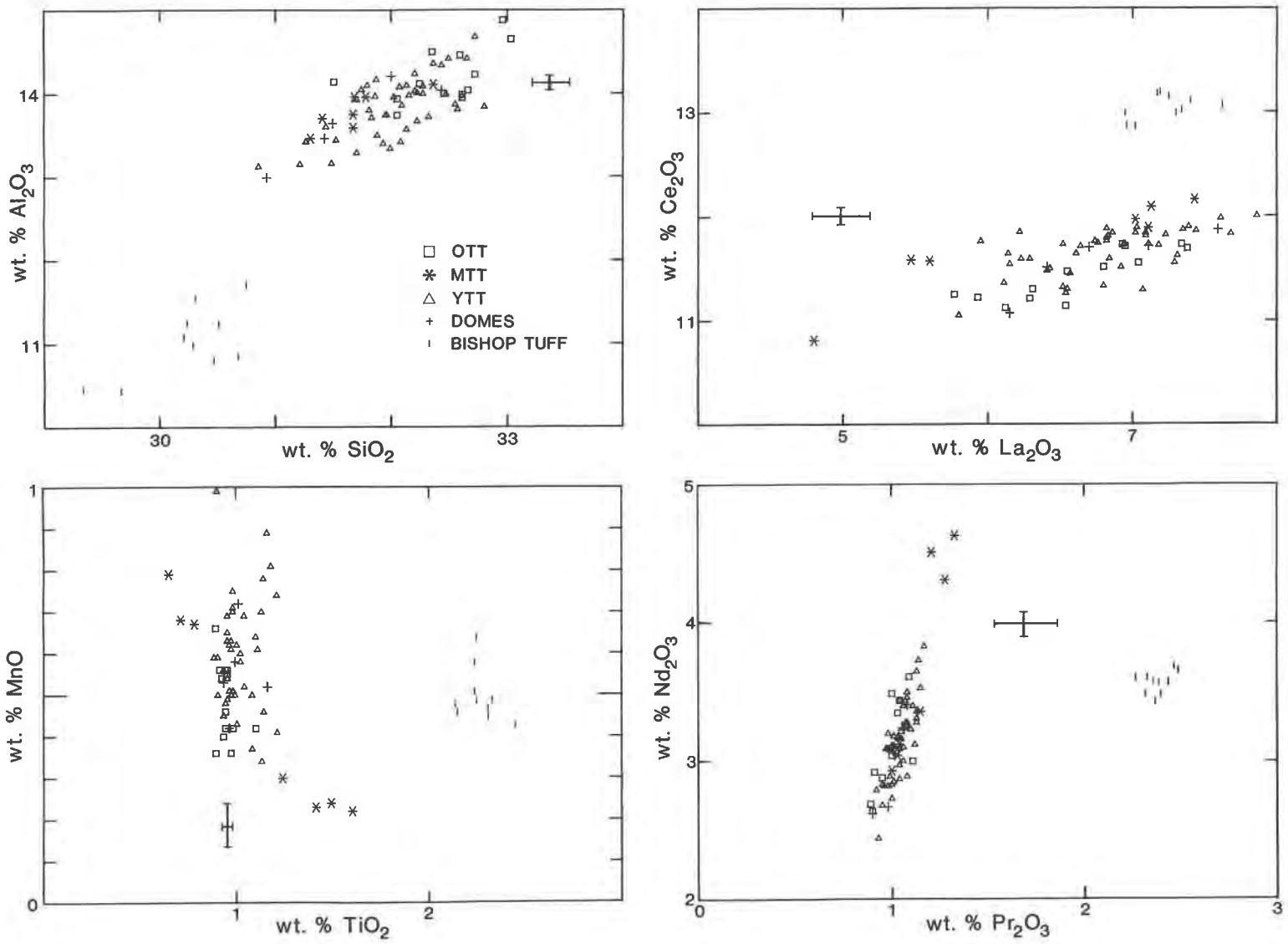

Fig. 6. Comparison of Toba Tuff allanites with those from the Bishop Tuff (Hildreth, 1977).

TABLE 4. Some crystal/liquid distribution coefficients for Toba allanite calculated from electron-microprobe and INAA data

	94A5	7	8
La	2691	2281	1165
Ce	1781	1557	1123
Sm	798	1187	1662
Eu	162	115	92
Tb	107	139	108
Yb	19	36	31
Lu	12	23	18

TABLE 5. Comparison of intensive parameters between the YTT and the Bishop Tuff

	YTT	Bishop Tuff
Temp (°C)	710–765	750–800
$-\log f_{O_2}$	14.5–16.5	12.5–15.5
P_{total} (kbar)	3.0–4.2	0.7–3.9
f_{H_2O} (bars)	360–480	200–600

Note: Fe-Ti oxide temperatures and f_{O_2} for the Bishop Tuff have been revised using data from Andersen and Lindsley (1985). Bishop Tuff data from Hildreth (1977) only includes allanite-bearing samples.

mostly as a function of temperature with perhaps some influence from P_{total} and P_{H_2O}. Allanite appears to be a late-stage volcanic mineral, crystallizing only in low-temperature magmas. Magmas below the critical allanite temperature often become stranded in the crust as plutonic bodies and continue to crystallize allanite until it eventually stops crystallizing in favor of epidote. Low-temperature epidote crystallization occurs as intergrowths with or epitaxial overgrowths on allanite (Deer et al., 1962; Gromet and Silver, 1983; Zen and Hammarstrom, 1984). Experimentally, magmatic epidote is stable between 600 and 700 °C in granodiorite at 8 kbar (Naney, 1983) and between 600 and 800 °C in trondhjemite at 15 kbar (Johnston and Wyllie, 1988). Thus, magmatic allanite exists only within a restricted range of temperatures, and its presence should be expected in calc-alkalic volcanic rocks with eruptive temperatures below 800 °C.

Comparisons with other allanite

Plutonic and metamorphic allanite vary greatly in composition (Gromet and Silver, 1983; Campbell and Ethier, 1984; Exley, 1980) largely because of hydration, alteration, and metamictization. Even fresh granitic rocks can have highly variable allanite compositions as a result of hydration and metamictization that occurs during slow cooling of the pluton. These phenomena are largely subordinate or lacking in volcanic allanites. Thus, the compositions of volcanic allanites are more representative of original compositions than plutonic allanites.

Allanites from the Bishop Tuff and from Toba are distinct chemically (Fig. 6). The Toba allanites have higher SiO_2, Al_2O_3, MnO, MgO, CaO, Y_2O_3, and ThO_2; TiO_2, FeO, and REEs are lower. This is not due to differing magma composition, as the Toba magmas have higher REE concentrations than the Bishop Tuff, but their allanites have lower REE abundances. Although physical conditions at which the Toba and Bishop Tuffs were erupted overlap (Table 5), the Toba magmas were generally cooler, at higher pressures, and less oxidizing. Thus, the difference in allanite composition between the Toba Tuffs and the Bishop Tuff is also probably a function of physical parameters of the magmas such as temperature, f_{O_2}, P_{total}, and P_{H_2O}.

CONCLUSIONS

(1) Allanite compositions in the Toba Tuffs vary with magma composition and temperature. (2) "Cross-over" patterns between the LREEs and HREEs on REE plots of Toba bulk-rock and glass samples is strong evidence for allanite fractionation. (3) Calculated allanite modes range from 0.016 to 0.035%; 0.052% allanite fractionation was necessary to produce the observed decreases in the LREE abundances of the YTT bulk-rock samples. (4) Below a critical temperature of about 800 °C, allanite may crystallize in silicic magmas; high abundances of REEs are not necessary.

ACKNOWLEDGMENTS

Research supported by National Science Foundation Grants EAR 82-06685 and EAR 85-11914. Scott Cornelius's help with the electron-microprobe analyses at Washington State University was instrumental. Editorial assistance from Bill Rose was greatly appreciated. Aka and Kalaika provided crucial field assistance.

REFERENCES CITED

Andersen, D.J., and Lindsley, D.H. (1985) New (and final!) models for the Ti-magnetite/ilmenite geothermometer and oxygen barometer. EOS, 66, 416.

Brooks, C.K., Henderson, P., and Rønsbo, J.G. (1981) Rare-earth partitioning between allanite and glass in the obsidian of Sandy Braes, Northern Ireland. Mineralogical Magazine, 44, 157–160.

Cameron, K.L. (1984) The Bishop Tuff revisited: New rare earth element data consistent with crystal fractionation. Science, 224, 1338–1340.

Campbell, F.A., and Ethier, V.G. (1984) Composition of allanite in the footwall of the Sullivan orebody, British Columbia. Canadian Mineralogist, 22, 507–511.

Chesner, C.A. (1985) Geochemistry of the Toba ignimbrites: Implications on silicic magma bodies, outflow patterns, and caldera collapse. EOS, 66, 1141.

Chesner, C.A., and Rose, W.I. (1987) Pre-eruptive conditions of magma bodies giving rise to the Toba Tuffs, Sumatra. U.S. Geological Survey Hawaii Symposium on How Volcanoes Work, Abstract Volume, 36.

Deer, W.A., Howie, R.A., and Zussman, J. (1962) Rock-forming minerals, vol. 1, ortho- and ring silicates, 333 p. Wiley, New York.

Dollase, W. (1971) Refinement of the crystal structures of epidote, allanite, and hancockite. American Mineralogist, 56, 447–464.

Drake, M.J., and Weill, D.F. (1972) New rare earth element standards for electron microprobe analysis. Chemical Geology, 10, 179–181.

Exley, R.A. (1980) Microprobe studies of REE-rich accessory minerals: Implications for Skye granite petrogenesis and REE mobility in hydrothermal systems. Earth and Planetary Science Letters, 48, 97–110.

Gromet, L.P., and Silver, L.T. (1983) Rare earth element distributions

among minerals in a granodiorite and their petrogenetic implications. Geochimica et Cosmochimica Acta, 47, 925–929.

Hildreth, E.W. (1977) The magma chamber of the Bishop Tuff: Gradients in temperature, pressure, and composition. Ph.D. thesis, 328 p. University of California, Berkeley, California.

Hildreth, W. (1979) The Bishop Tuff: Evidence for the origin of compositional zonation in silicic magma chambers. Geological Society of America Special Paper 180, 43–75.

Johnston, A.D., and Wyllie, P.J. (1988) Constraints on the origin of Archean trondhjemites based on phase relationships of Nuk gneiss with H_2O at 15 kbar. Contributions to Mineralogy and Petrology, 100, 35–46.

Knight, M.D., Walker, G.P.L., Elwood, B.B., and Diehl, J.F. (1986) Stratigraphy, paleomagnetism, and magnetic fabric of the Toba Tuffs: Constraints on the sources and eruptive styles. Journal of Geophysical Research, 91, 355–382.

Marel, H.W. van der. (1948) Volcanic glass, allanite, and zircon as characteristic minerals of the Toba rhyolite at Sumatra's east coast. Journal of Sedimentary Petrology, 18, 24–29.

Michael, P.J. (1983) Chemical differentiation of the Bishop Tuff and other high-silica magmas through crystallization processes. Geology, 11, 31–34.

——— (1984) Chemical differentiation of the Cordilleran Paine granite (southern Chile) by in situ fractional crystallization. Contributions to Mineralogy and Petrology, 87, 179–195.

Naney, M.T. (1983) Phase equilibria of rock forming ferromagnesian silicates in granitic systems. American Journal of Science, 283, 993–1033.

Peacor, D.R., and Dunn, P.J. (1988) Dollaseite-(Ce) (magnesium orthite redefined): Structure refinement and implications for $F + M^{2+}$ substitutions in epidote-group minerals. American Mineralogist, 73, 838–842.

Zen, E., and Hammarstrom, J.M. (1984) Magmatic epidote and its petrological significance. Geology, 12, 515–518.

Manuscript received June 23, 1988
Manuscript accepted March 16, 1989